Morphodynamics and Sedimentology of Channels in Tidal Bars and Tidal Flats*

Sergio Fagherazzi[1], Giulio Mariotti[1], and Tao Sun[2]

Search and Discovery Article #50519 (2011)
Posted November 30, 2011

*Adapted from extended abstract prepared in conjunction with poster presentation at AAPG International Conference and Exhibition, Milan, Italy, October 23-26, 2011

[1]Department of Earth Sciences, Boston University, Boston, MA (sergio@bu.edu)
[2]Exxon Mobil Upstream Research Company, Houston, TX

Abstract

Deltas and estuaries are often characterized by tidal bars and tidal flats that collect and store sediments discharged by rivers. Both landforms are dissected by channel incisions that are critical for the redistribution of sediment and water and for the general evolution of these sedimentary deposits. Tidal flow concentrates in depressions leading to higher shear stresses thus promoting bottom erosion. At the same time a decrease of shear stress in higher locations promotes sediment deposition and accumulation. This combined mechanism is responsible for the formation of tidal incisions and the alternation of bars and channels in tidal environments. However, little is known about the complex feedbacks between tidal forcing and the formation of tidal channels. In fact, during a tidal cycle, the estuarine/deltaic bottom experiences a large range of velocities and water elevations, so that it is difficult to determine which event (or series of events) is responsible for channel formation. Here we compare extensive field measurements in Willapa Bay, Washington State, and Plum Island Sound, Massachusetts, two mesotidal environments in the United States. When the tidal flat is submerged, ebb-flood asymmetries in suspended sediment concentration are present. These asymmetries produce ebb and flood pathways with distinct morphological characteristics. We show that sediment deposition and erosion is clearly affected by this variability of flow along the bar/flat system. The redistribution of momentum between tidal bar and tidal channel leads to patterns of deposition and erosion that create distinctive layers of coarse and fine sediments, whose size and location are a function of tidal hydrodynamics and sediment availability.

Introduction

Tidal deltas and estuaries often present a series of elongated tidal bars both in the delta foreset and within the estuary. A succession of bars and channels dissect the bottom of the delta front with differences in elevations up to 10 m. Tidal bars redistribute tidal fluxes between shallower and deeper areas. A hydrodynamic mechanism already presented in Fagherazzi and Furbish (2002) concentrate the tidal flow in the trough leading to higher shear stresses thus promoting bottom erosion. At the same time a decrease of tidal flow on top of the bar promotes sediment deposition and accumulation. This combined mechanism is responsible for the formation of tidal bars and the alternation of bars and channels in tidal environments.

However, little is known about the complex feedbacks between tidal forcing and the formation of tidal bedforms. In fact, during a tidal cycle, the bottom experiences a large range of velocities and water elevations, so that it is difficult to determine which event (or series of events) is responsible for tidal bar formation. Moreover, sediment deposition and erosion is clearly affected by this variability of flow along the estuary. Segregation of coarse and fine sediments in selected locations within the tidal bar system can produce a unique bottom stratigraphy rich in potential reservoirs, which can be of great interest for oil and gas exploration. Our hypothesis is that the redistribution of momentum between tidal bar and tidal trough leads to patterns of deposition and erosion that create distinctive layers of coarse and fine sediments, whose size and location are a function of tidal hydrodynamics and sediment availability.

Study Site

Plum Island Sound Massachusetts, USA (Figure 1) is a shallow tide-dominated estuary that experiences semi-diurnal tides with mean range of 2.6 m increasing to 3.2 m during spring tide conditions. The Parker, Rowley, and Ipswich Rivers flow into Plum Island Sound with a total freshwater discharge of 89 x 106 m3, which when computed over a half tidal cycle is several orders of magnitude smaller than the saltwater tidal prism (3.0 x 107 m^3). More than half of the freshwater influx to the estuary enters via the Ipswich River at the lower end of the Sound. This condition coupled with the large tidal range and relatively shallow nature of the Sound produces a well-mixed, saline estuary. Dams along the rivers combined with well-vegetated watersheds explain why little riverine sediment is contributed to the estuary. Likewise, the coastal ocean has a very low suspended sediment concentration and thus delivers little mud to the Sound or to the surrounding salt marshes.

Field Methods

A topographic survey of the morphology of the tidal bars was performed in September 2009 using a Laser Total Station. The survey determined the elevation of the bar along the three transects indicated in Figure 2 (transects A-G, H-I, J-K). The bottom elevation was measured every 5-10 m depending on local morphological features. Twelve sediment samples were taken along the transect A-G to determine sand granulometry and percentage of fine sediments (silt and clay).

Two deployments were performed in summer 2010. The first deployment took place from 7/15/10 to 8/13/10. In this deployment an array of instruments was located at the buoys A B C D in Figure 2. At buoy A, we deployed a Nortek Aquadopp current profiler (ADCP) upper looking with a D &A Optical Backscattering Sensor (OBS 3+) located 30cm above the bed. The ADCP measured water velocity along the vertical every 10cm with a blanking distance of 10 cm. The instrument recorded the velocity every 30min for the deployment duration. At the Buoy B we deployed a second ADCP with OBS and a Nortek Vector Acoustic Velocimeter (ADV). The ADV was mounted on a frame and pointed toward the bed with the sampling volume 15 cm from the bottom. The ADV recorded water velocity at 32 Hz every 30 min with a burst of 4096 points. At buoy C we deployed a third ADCP with a Tritech Altimeter PA500-6. The Altimeter is deployed 67 cm from the bottom and measure changes in bottom elevation with a resolution of 1 cm. At buoy D we deployed a fourth ADCP with OBS and a second ADV with the same configuration of buoy 2. All ADCPs also measured waves every hour at 2Hz with a burst of 512 points. During the second deployment, from 08/13/10 to 09/11/10, the ADCP at buoy A was moved to buoy F and the ADCP at buoy D was moved at buoy E with same configuration and sampling characteristics. The goal of the second deployment was to study the tidal hydrodynamics along the transect D-G in Figure 2.

Field Results

The results of the topographic survey are reported in Figure 2. Two ebb channels are dissecting the tidal bar (see transect A-G) the channels are 1.5 m deep and 50-80 m wide. The channels are also present along transect I-H, located to the north, with similar depth but larger cross section. The same channels can also be identified along transect J-K, although their depth decrease considerably (less than 1 m). Two broad concavities interfinger the ebb channels and surround the two buoys D and F in Figure 2. The concavities are delimited by levees up to 0.5 m high that separate them from the ebb channels. The concavities disappear to the north, along the transect I-H, and are more pronounced to the south, along the transect J-K. Here it is almost impossible to distinguish the ebb channels from the concavities, having comparable width and depth. Ebb channels reach the lowest elevation in the north part and become shallower until disappearing in the southern part. On the contrary, the concavities are deep in the southern part and are not present in the northern part.

We collected and analyzed historical images of the tidal bar to understand the formation of the alternate channel-convexity morphology and its evolution in time. In Figure 3 we compare four aerial images taken between 1995 and 2008. We note the formation and extension of the second channel tidal in time (buoy E in Figure 2). Sediments are transported in the channel during ebb and then laterally deposited in levees and splays. These topographic heights might prevent the water to flow back in the channels during flood, and actively create segregated patterns for the flow.

In Figure 4 we report the bottom velocity (last bin of the ADCP between 10 and 20 cm of elevation) as a function of time for two tidal cycles. The velocity is shown for buoy D, at the center of the first concavity, and for buoy C in the channel. The results show that the flow at both locations has same magnitude both in flood and in ebb and that the velocities are of the same order of magnitudes for three tidal cycles. However, during the second ebb the bottom velocity dramatically increased on the concavity, possibly triggering large sediment transport. These preliminary data show how transient flows might have a strong influence on bar morphology and stratigraphy.

Modeling Ebb-Flood Channels on the Tidal Bar

While the bar boundaries with the main channel are relatively stable, the topography of the bar is extremely dynamic (Figure 3). The channels incising the bar are continuously reworked, suggesting that they do not reach equilibrium or that their equilibrium is very unstable.

Current measurements indicate that the ebb channels do not experience significant velocity asymmetries. This suggests that tidal asymmetry is not the driving mechanism for the ebb (flood) channel evolution. Other asymmetries or feedbacks should drive the evolution of the channels. Here we explore the hypothesis that the ebb channel evolution is a consequence of an initial asymmetric topography of the bar. Figure 2 shows that the northern part of the sand bar is characterized by sediment relief, while the southern part has lower elevation.

To test our hypothesis we use the hydro-morphodynamic model Delft3D (Lesser et al., 2004). The model is run in 2D, using van Rijn (1984) equations for bed load transport and the advection diffusion equation for suspended load transport. Here we made the assumption that the flow on the inner part of the bar is not affected by the lateral presence of the main channel. The presence of the main channel is affecting the bar only at the upper (northern) and lower (southern) edges of the bar. With this assumption we can consider a simplified geometry and hydrodynamic setting.

The model domain consists of a flat surface placed at -2 m respect to the MSL, representing an idealized tidal bar. At the upper and lower boundary of the tidal bar a 5m deep areas are present. These areas represent the main channel, and have the purpose to create a buffer zone for the boundary conditions. Since we neglect the lateral influence of the main channel, no flux conditions are imposed at the lateral boundary (Figure 5). We made the further assumption that the level and the mean barotropic gradient on the tidal bar are imposed by the flow in the main channel. To calculate this barotropic gradient, a simplified procedure is used. We assume that the tide propagates as a standing wave, which implies the following relationship:

$$Q = A\frac{\partial \xi}{\partial t}$$

where Q is the water discharge, A is water surface area, and ξ is the water level. We then assume that the flow is concentrated in the main-channel. Finally, assuming that local acceleration and inertia are negligible, we apply the Chezy equation to compute the baroptropic gradient along the main channel:

$$\frac{\partial \xi}{\partial x} = \frac{U^2}{C^2}\frac{1}{d_c} = \frac{Q^2}{C^2}\frac{1}{{d_c}^3} = \frac{A^2}{C^2}\left(\frac{\partial \xi}{\partial t}\right)^2 \frac{1}{(\xi - z_c)^3}$$

where C is the Chezy coefficient, d_c is the water depth in the main channel, z_c is the channel elevation (5m). For simplicity, we impose a sinusoidal water level ($\partial\xi/\partial t$), with an amplitude of 1.5 m. The resulting barotropic gradient is ebb-flood symmetric, and has a maximum at a water depth -1m respect to the MSL (Figure 6).

Finally, we introduce an asymmetry in the bar topography. A mound of sediment 1.5 m high (respect to the tidal bar) and 20 m long is placed at one edge of the bar (Figure 6). This mound can be thought to represent the sill of the levees of other ebb-flood channels. This situation is common, given the articulated geometry of sand bodies. In addition, we introduce a perturbation on the mound which represents the incipient incision of a channel.

The incision of the mound grows in time (Figure 6). The depth of the incision increases, as suggested by the model of Fagherazzi and Furbish (2001). In addition, the channel progrades are toward the ebb direction (i.e. toward the lower part of the bar). During this progradation, the channel forms lateral levees and a centerline deposit at its end. The progradation of the channel takes place predominantly during the ebb phase, while during the flood phase the topography varies little.

The simulations suggest that the progradation during ebb is the result of a jet expansion (from the channelized flow to the open bar flow). Because of the jet expansion, the flow reduces its transport capacity and deposit the sediment entrained in the ebb channel. This mechanism is analogous to a river mouth bar and levees formation. During flood instead, the flow is contracting and does not trigger the same jet expansion in the flood direction.

In conclusion, we suggest that the progradation of the channel is the result of a jet asymmetry (expansion-contraction) between ebb and flood.

References

Fagherazzi, S., and D.J. Furbish, 2001, On the shape and widening of salt marsh creeks: Journal Geophysical Research, v. 106/C1 , p. 991-1005.

Lesser, G., J. Roelvink, J. Van Kester, and G. Stelling, 2004, Development and validation of a three-dimensional morphological model: Coastal Engineering, v. 51, p. 883-915.

van Rijn, L.C., 1984, Sediment transport; part I, Bed load transport: Journal Hydraulic Engineering, v. 110, p. 1431-1456.

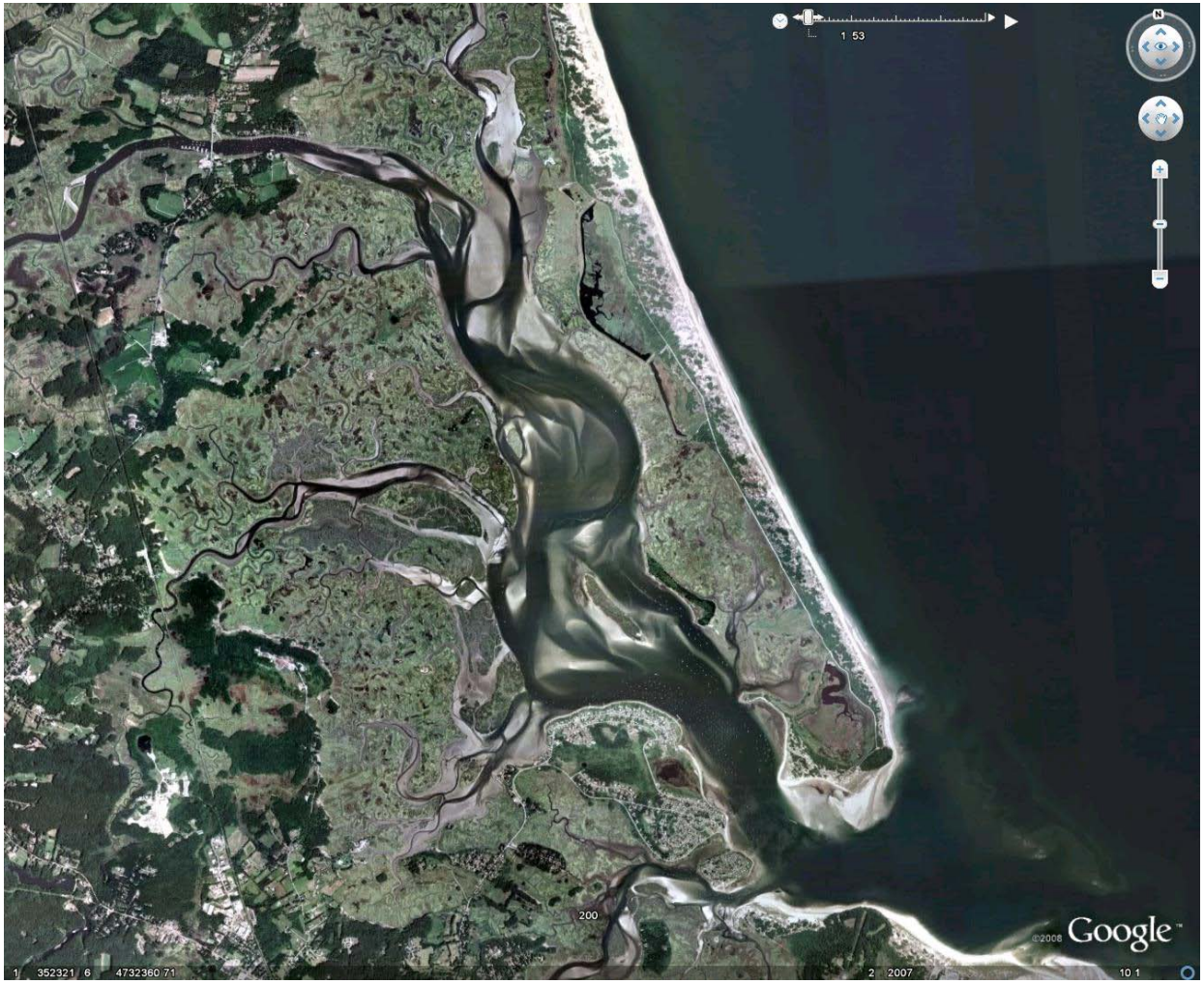

Figure 1. Study site: Plum Island Sound, Massachusetts. A tidal bar complex is visible at low tide.

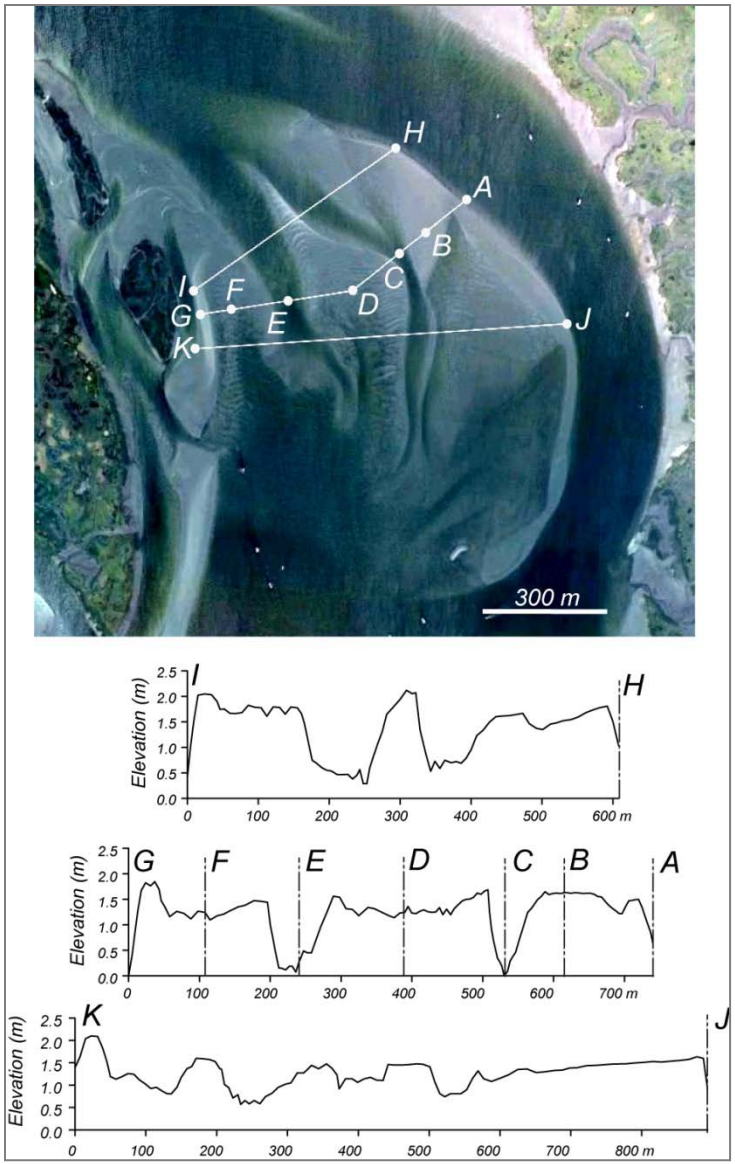

Figure 2. Tidal bar studied in this project and topographic transects A-G, H-I and J-K.

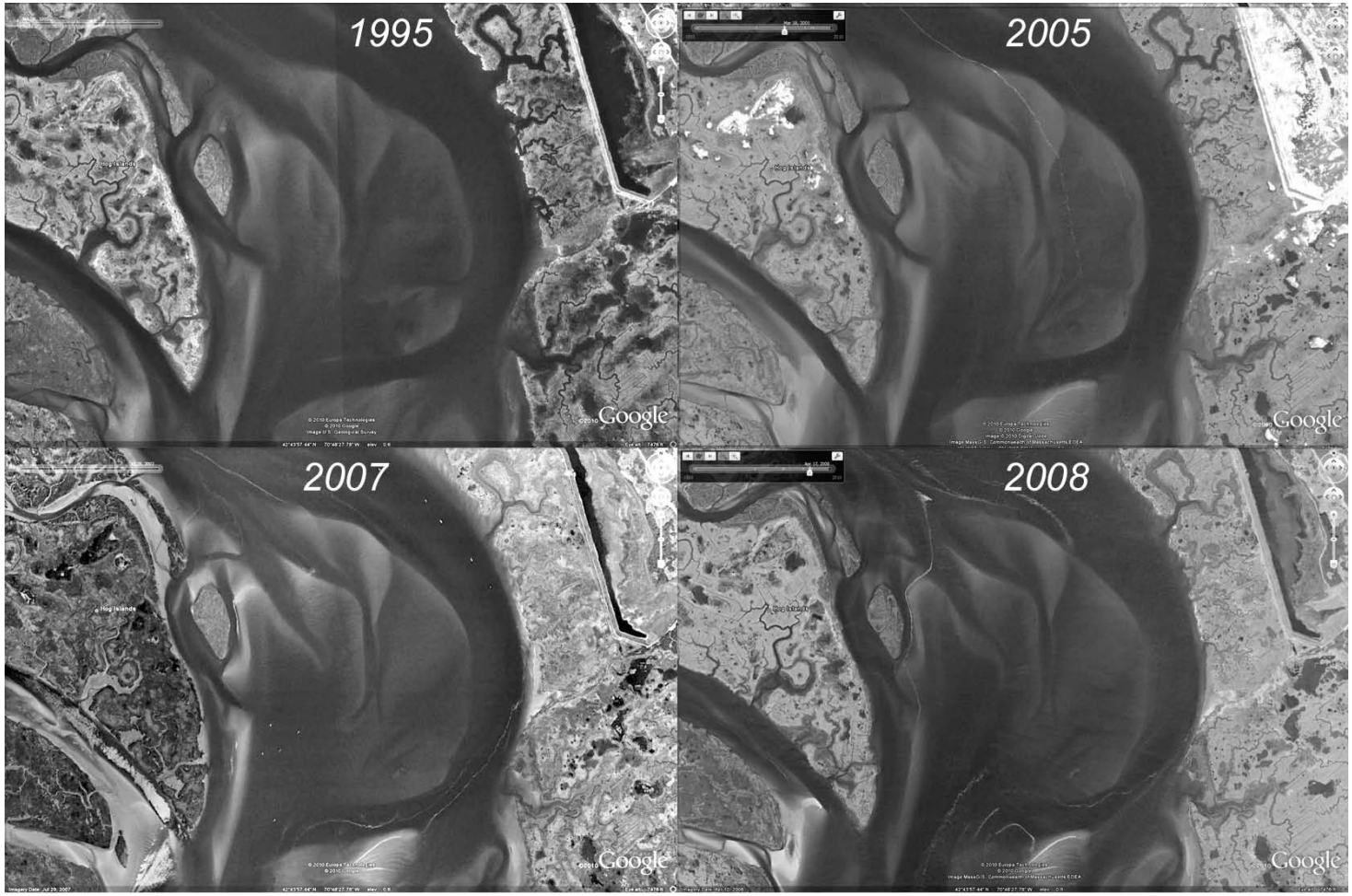

Figure 3. Evolution of the studies tidal bar from 1995 to 2008.

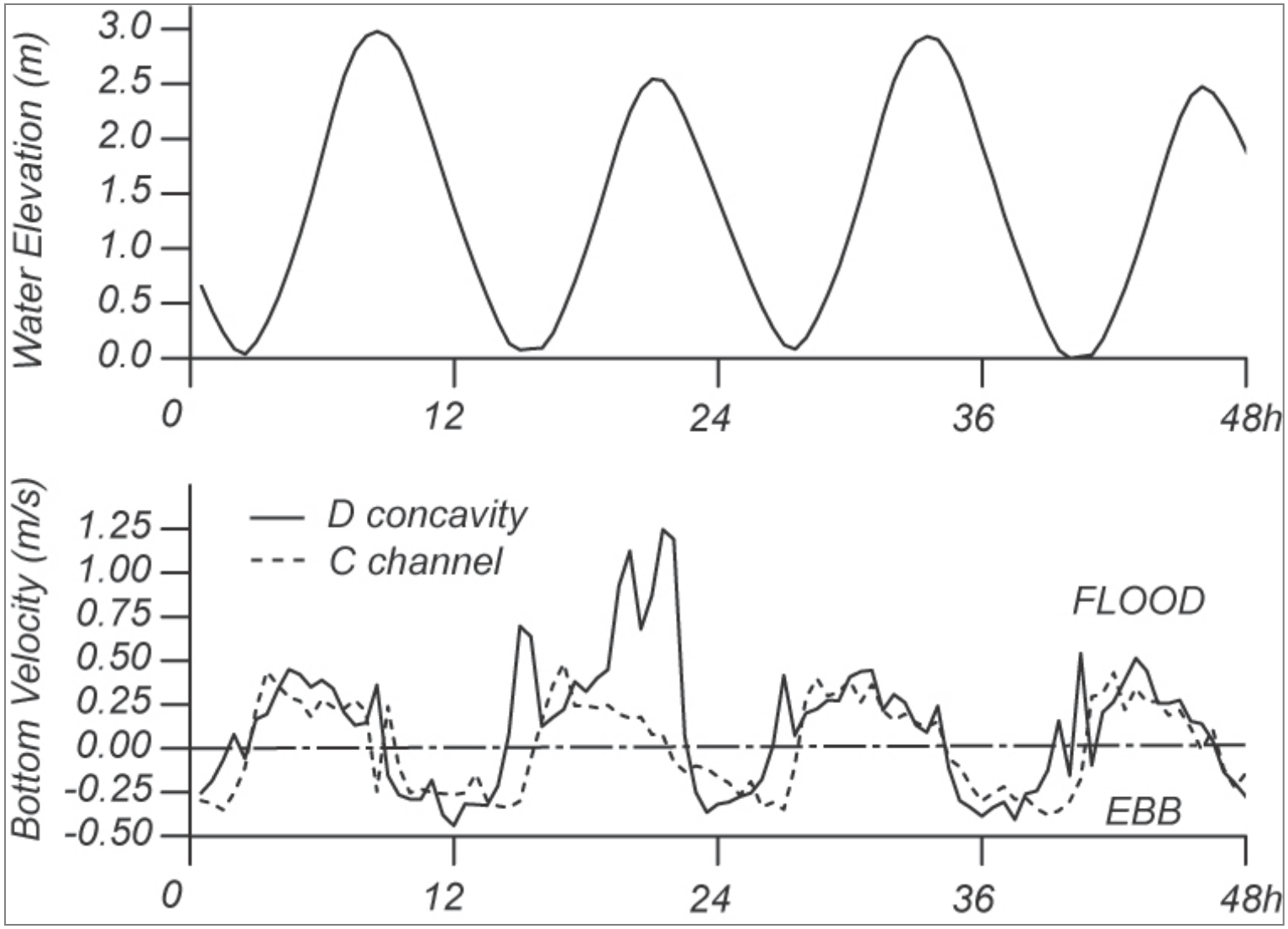

Figure 4. Bottom velocity for four tidal cycles in the channel (buoy C in Figure 2) and in the nearby concavity (buoy D in Figure 2).

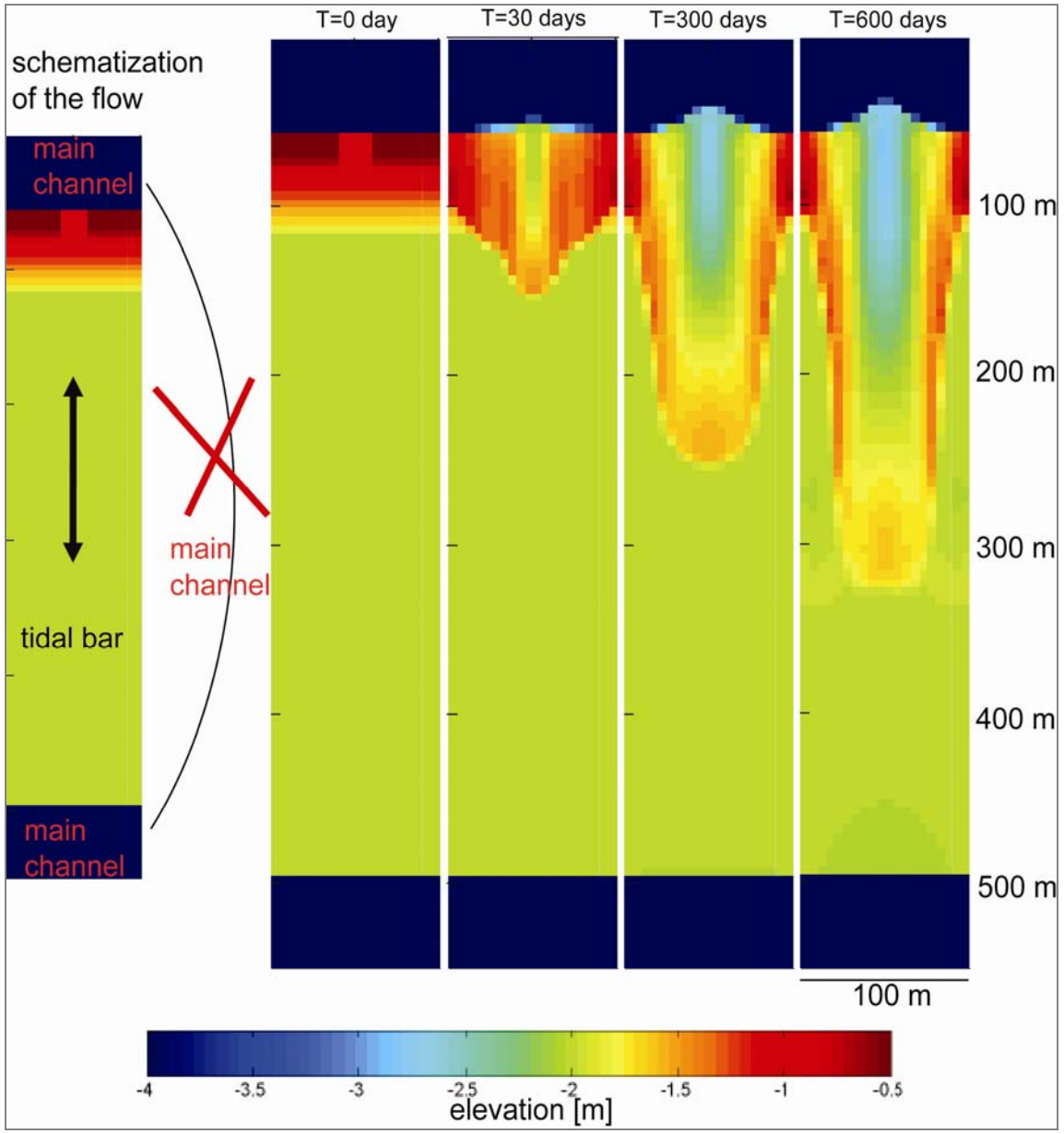

Figure 5. Formation and evolution of an ebb-flood channel on a tidal bar. The channel forms by dissecting the bar surface and depositing the eroded sediments on lateral levees and on a mouth ridge.

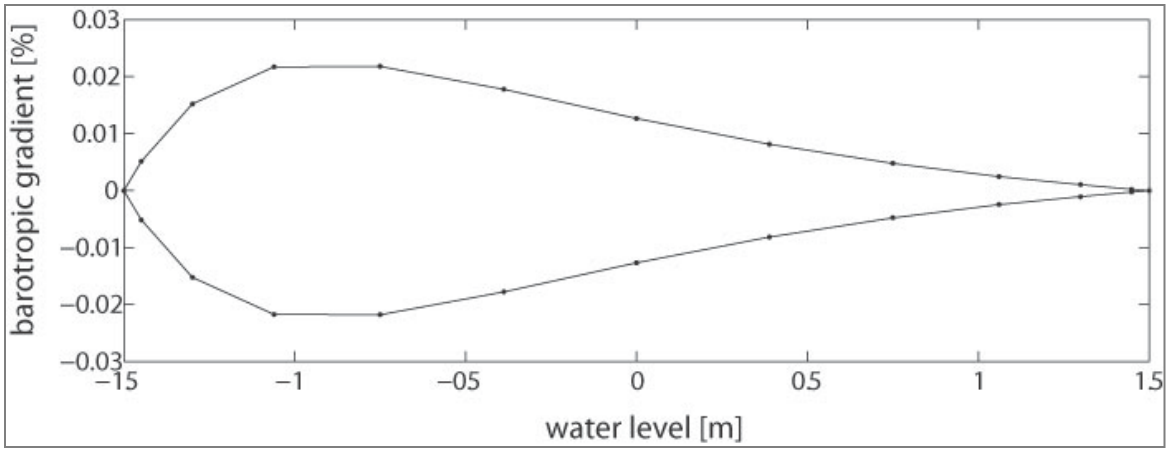

Figure 6. Barotropic gradient imposed as a boundary condition for the model simulations reported in Figure 5.